environmental microbiology

Environmental Microbiology (2017) **19**(9), 3500–3513 doi:10.1111/1462-2920.13834

Recognition cascade and metabolite transfer in a marine bacteria-phytoplankton model system

Bryndan P. Durham,[1†] Stephen P. Dearth,[2] Shalabh Sharma,[3] Shady A. Amin,[4‡] Christa B. Smith,[3] Shawn R. Campagna,[2] E. Virginia Armbrust[4] and Mary Ann Moran[3]*

[1]*Department of Microbiology, University of Georgia, Athens, GA, USA.*

[2]*Department of Chemistry, University of Tennessee, Knoxville, TN, USA.*

[3]*Department of Marine Sciences, University of Georgia, Athens, GA, USA.*

[4]*School of Oceanography, University of Washington, Seattle, WA, USA.*

Summary

The trophic linkage between marine bacteria and phytoplankton in the surface ocean is a key step in the global carbon cycle, with almost half of marine primary production transformed by heterotrophic bacterioplankton within hours to weeks of fixation. Early studies conceptualized this link as the passive addition and removal of organic compounds from a shared seawater reservoir. Here, we analysed transcript and intracellular metabolite patterns in a two-member model system and found that the presence of a heterotrophic bacterium induced a potential recognition cascade in a marine phytoplankton species that parallels better-understood vascular plant response systems. Bacterium *Ruegeria pomeroyi* DSS-3 triggered differential expression of >80 genes in diatom *Thalassiosira pseudonana* CCMP1335 that are homologs to those used by plants to recognize external stimuli, including proteins putatively involved in leucine-rich repeat recognition activity, second messenger production and protein kinase cascades. Co-cultured diatoms also downregulated lipid biosynthesis genes and upregulated chitin metabolism genes. From differential expression of bacterial transporter systems, we hypothesize that nine diatom metabolites supported the majority of bacterial growth, among them sulfonates, sugar derivatives and organic nitrogen compounds. Similar recognition responses and metabolic linkages as observed in this model system may influence carbon transformations by ocean plankton.

Received 25 January, 2017; accepted 13 June, 2017. *For correspondence: E-mail: mmoran@uga.edu; Tel. 706-542-6481; Fax 706-542-5888. Present addresses: †School of Oceanography, University of Washington, Seattle, WA, USA; ‡Department of Biology, New York University Abu Dhabi, Abu Dhabi, UAE.

Introduction

The fate of carbon in marine environments is influenced by associations between co-occurring heterotrophic bacteria and phytoplankton (Azam and Malfatti, 2007). Such associations include trophic links (Azam *et al.*, 1983; Obernosterer and Herndl, 1995) as well as chemical communication and exchange (Kerkhof *et al.*, 1999; Mayali and Azam, 2004; Geng and Belas, 2010; Amin *et al.*, 2012). Deciphering the nature of these associations is critical given the impact of marine plankton on biogeochemical cycling and climate regulation.

An improved understanding of bacteria-phytoplankton interactions will require knowledge of the molecules exchanged between the cells and information on whether or not specific recognition mechanisms play a role. The configuration of such interactions is likely to be extremely diverse, since examples of bacteria-phytoplankton relationships vary broadly from pathogenic to mutualistic (Mayali and Azam, 2004; Seyedsayamdost *et al.*, 2011; Xie *et al.*, 2013; Amin *et al.*, 2015; Aharonovich and Sher, 2016; Mayers *et al.*, 2016; Segev *et al.*, 2016). Most direct interactions are proposed to take place in the phycosphere, a diffusive boundary layer immediately surrounding phytoplankton cells that is enriched in organic matter (Bell and Mitchell, 1972). In some cases, marine bacteria have been shown to physically attach to phytoplankton (Bidle *et al.*, 2002; Gärdes *et al.*, 2011; van Tol *et al.*, 2017) while in others the interactions occur via diffusible molecules (Manefield *et al.*, 2002; Amin *et al.*, 2012; 2015; Paul *et al.*, 2012; Seyedsayamdost *et al.*, 2014).

Some diffusible molecules exchanged in the phycosphere, such as indole-3-acetic acid (Amin *et al.*, 2015; Segev *et al.*, 2016), are analogous to those exchanged between land plants and soil bacteria, indicating potential parallels in signaling and interaction mechanisms (Hughes and Sperandio, 2008). In plant models of bacterial

recognition, leucine-rich repeat (LRR) proteins located either at the cell surface or in the cytoplasm play key signaling roles in plant immunity and development, including hormone binding, pathogen defense, nodulation and embryogenesis (Diévart and Clark, 2004; Yue *et al.*, 2012). Downstream signal cascades are widely used by plants to further relay responses, including the calcium-dependent protein kinase (CDPK) and the mitogen-activated protein kinase (MAPK) pathways (Ligterink and Hirt, 2001; Vadassery and Oelmüller, 2009). These signaling networks direct and modulate the plant response to bacterial presence as well as other external stimuli, leading to outcomes such as cell cycle changes, metabolic rearrangements and defense-related gene activation.

Transcription and metabolome assays can be used to address the basis of ecological associations between bacteria and phytoplankton through identification of the set of genes and metabolic pathways that are differentially regulated when the microbes co-occur (Seyedsayamdost *et al.*, 2011; Paul *et al.*, 2012; Amin *et al.*, 2015). Evidence for induction of putative recognition pathways in phytoplankton transcriptomes might indicate a capability to detect the presence of bacteria and activate interaction mechanisms. Shifts in expression of genes mediating metabolic pathways could provide clues regarding the substrates or secondary metabolites exchanged between microbial cells (Wang *et al.*, 2014; Amin *et al.*, 2015; Durham *et al.*, 2015).

Here, we study a model microbial system consisting of diatom *Thalassiosira pseudonana* and bacterium *Ruegeria pomeroyi* DSS-3. The diatom requires an exogenous source of vitamin B_{12}, which is provided by the bacterium, while the heterotrophic bacterium is dependent on organic carbon and a usable nitrogen source from the diatom (Durham *et al.*, 2015). A mutualism of this type is likely to be commonplace in the ocean given that B_{12} auxotrophy is widespread among eukaryotic phytoplankton (Croft *et al.*, 2005; Helliwell *et al.*, 2011). Further, both members of the model system represent taxa important in the ocean. Bacteria in the Roseobacter lineage are ubiquitously distributed in surface waters and consistently found in association with diatoms (González *et al.*, 2000; Suzuki *et al.*, 2001; Pinhassi *et al.*, 2004; Grossart *et al.*, 2005; Amin *et al.*, 2012), and diatoms are one of the dominant primary producers in coastal and upwelled ocean waters (Nelson *et al.*, 1995). Durham and colleagues (2015) described a novel metabolite, 2,3-dihydroxypropane-1-sulfonate (DHPS), involved in carbon transfer using this model system. In this analysis, we focus on the breadth of transcriptional and metabolomic signals to ask two questions: What metabolites sustain the trophic link between this microbial autotroph and heterotroph? And to what extent does metabolite exchange occur through passive release and uptake versus through the influence of microbe-microbe interactions?

Results

R. pomeroyi DSS-3 and B_{12}-limited *T. pseudonana* CCMP1335 were grown together and individually, the latter serving as controls. In co-culture with the bacterium, *T. pseudonana* reached growth rates comparable to those in the mono-culture supplemented with exogenous B_{12} (0.78 d^{-1} and 0.75 d^{-1} respectively; ANCOVA, $F = 0.99$, Brand and Guillard, 1981), and values of the photosynthetic parameter F_v/F_m were similar (0.561 and 0.532 respectively). Bacteria grew to fourfold higher numbers in the co-culture compared with inoculation level (Fig. 1, Supporting Information Fig. S1). Microscopic examination of the cultures during exponential growth of the diatom revealed little surface attachment of *R. pomeroyi* to *T. pseudonana* cells, ranging from none to one or two per diatom. Transcriptome and metabolome analyses conducted at 8 h (bacteria and diatom) and 56 h (diatom) were used to compare mono- versus co-cultures for evidence of potential metabolic and ecological interactions.

Diatom recognition response

The diatom transcriptome showed little response to co-culture conditions at the first time point, 8 h after introduction of the bacterium, with only five *T. pseudonana* genes differentially regulated compared with the axenic mono-culture (Supporting Information Table S1). However, by the 56 h time point, exponentially growing co-cultured *T. pseudonana* differentially regulated 492 genes as compared

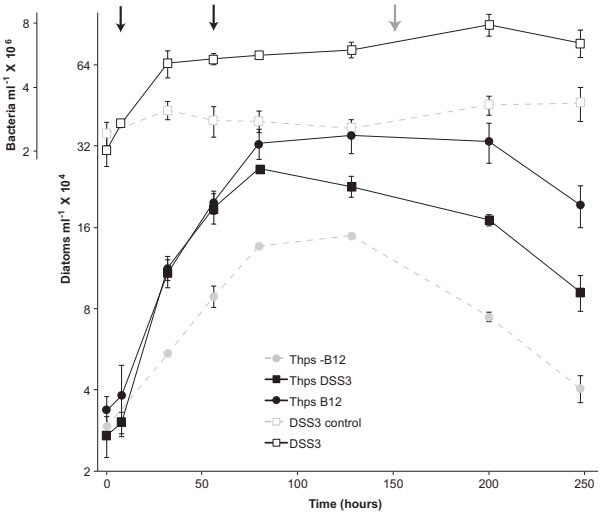

Fig. 1. Recovery of *Thalassiosira pseudonana* growth by addition of exogenous B_{12} (black filled circles) or *Ruegeria pomeroyi* DSS-3 (black filled squares) compared with a B_{12}-limited control (grey filled circles), and *R. pomeroyi* cell numbers in co-culture with *T. pseudonana* (black open squares) or in no-substrate controls (grey open squares). Black arrows indicate times when transcriptomes and metabolomes were analysed. Grey arrow indicates the time of culture transfer (see Supporting Information Fig. S5). Error bars represent the standard deviation of triplicate cultures.

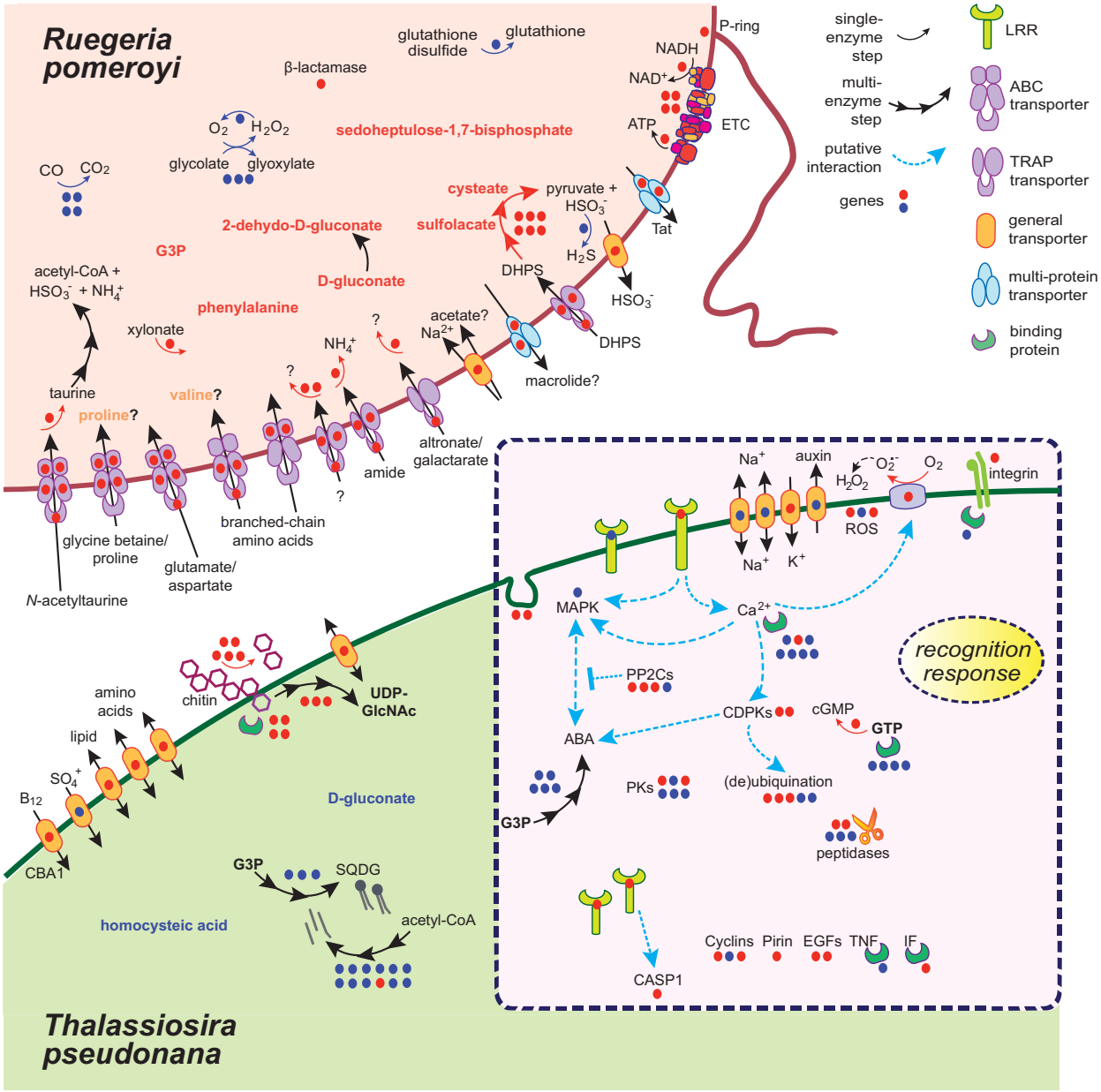

Fig. 2. Schematic of the *Ruegeria pomeroyi* DSS-3 and *Thalassiosira pseudonana* transcriptome and metabolome changes. Data for *R. pomeroyi* and *T. pseudonana* were analysed after 8 h and 56 h respectively (Fig. 1). Red dots and arrows indicate upregulation of genes and pathways, respectively, in co-culture versus mono-culture, while blue dots and arrows indicate downregulation. Detected intracellular metabolites are indicated in bold font, with red indicating significantly higher concentrations in co-culture versus mono-culture and blue indicating significantly lower concentration in co-culture (Fig. 4). Transporters with bidirectional arrows signify that direction of substrate movement is not known. ETC: electron transport chain; Tat: twin-arginine translocation; ABA: abscisic acid; PKs: protein kinases; G3P: glycerol-3-phosphate; ROS: reactive oxygen species; EGFs: epidermal growth factors; TNF: tumor necrosis factor; IF: interferon; SQDG: sulfoquinovosyl diacylglycerol. Additional definitions can be found in Tables 1 and 2.

with the B_{12}-replete axenic control (4.3% of the genome, 174 upregulated and 318 downregulated; Supporting Information Table S2). Of these, 209 had functional annotations (70 upregulated and 139 downregulated; Supporting Information Table S2). The B_{12} acquisition gene CBA1 (Bertrand *et al.*, 2012) was the only gene upregulated at both time points.

Gene expression comparisons between diatoms in co-cultures versus axenic mono-cultures at the 56 h time point indicated that over 80 differentially expressed *T. pseudonana* genes had annotations suggesting recognition and signaling functions (Fig. 2, Supporting Information Table S2). Four were putative LRR receptor proteins (upregulated Tp5595, Tp25675, Tp20707; downregulated Tp24726).

Nine genes differentially transcribed in co-culture had calcium-binding domains or were annotated as calcium-responsive genes (Fig. 2, Table 1). Genes encoding three ion channels (Tp3092, K^+ channel; Tp711, bile acid-Na symporter; Tp4725, Na-H antiporter) and an NADPH oxidase (Tp11375) were also differentially expressed.

One MAPK gene (Tp9710) was differentially expressed out of five genes with this annotation in the genome, and it was downregulated ninefold in co-culture. In plants, MAPK signaling can be negatively regulated by signal transduction regulators including isoprenoid hormones such as abscisic acid (Danquah *et al.*, 2014) and protein phosphatase family 2C (PP2C)-type phosphatases (Schweighofer *et al.*, 2004). In the diatom transcriptome, five genes involved in the synthesis of isoprenoids and four genes encoding PP2Cs were differentially regulated in co-culture (Fig. 2, Table 1).

Additional differentially expressed genes with homology to those involved in downstream transduction and regulation in plant signaling cascades included those predicted to encode ubiquitination/deubiquitination enzymes that target proteins for degradation, receptors and receptor-associated factors, peptidases, an interferon regulator, an integrin and guanylate cyclase which synthesizes second messenger cGMP in response to intracellular calcium levels (Fig. 2, Table 1, Supporting Information Table S2). Eleven genes with predicted involvement in intracellular trafficking were significantly upregulated or downregulated. These included upregulated homologs to clathrin and epsin, proteins typically indicative of endocytosis (Ford *et al.*, 2002). Thirteen differentially expressed genes had annotations related to cell growth and cell cycle regulation, including three cyclins, two regulators of chromosome condensation, two proteins containing epidermal growth factor (EGF) domains, a metacaspase and pirin (Fig. 2, Table 1).

Diatom differential regulation of metabolism genes

Nearly 90 genes involved in metabolism and transport were differentially expressed 56 h after bacterial inoculation (Supporting Information Table S2, Fig. 2). Three genes associated with sulfo/glycerolipid biosynthesis were downregulated (Durham *et al.*, 2015), as were twelve genes involved in fatty acid biosynthesis. The diatom urea cycle gene carbamoyl phosphate synthase (*unCPS*; Tp40323) was downregulated threefold (Supporting Information Table S2). Twelve genes mediating chitin metabolism or containing chitinase or chitin-binding domains were upregulated by *T. pseduonana* in co-culture, as was a component of a putative UDP-GlcNAc transporter system (Tp2088) (Table 1).

Bacterial differential regulation of transport and metabolism genes

To detect transcriptional changes related to substrate uptake, *f*/2 medium with no carbon source was used in the mono-culture bacterial controls. Analysis of transcriptional

Table 1. Selected list of differentially expressed genes in *Thalassiosira pseudonana* (76 out of 492; 209 of which have functional annotations) highlighting those involved in signaling and recognition responses, chitin metabolism and transport when co-cultured with bacterium *Ruegeria pomeroyi* DSS-3 ($n = 2$) relative to B_{12}-replete mono-culture ($n = 2$) after 56 h of growth.

General function	Locus tag	Description	Fold change
Leucine-rich repeat	5595	LRR, transmembrane	**3.2**
(LRR) receptors	20707	LRR, cytoplasmic	**3.4**
	24726	LRR, transmembrane	−3.6
	25675	LRR, cytoplasmic	**3.0**
Calcium-dependent	14490	CDPK	**2.4**
protein kinase (CDPK) pathway	36897	CDPK	**4.4**
and calcium-binding proteins	7282	Calcium-binding EF-hand (calmodulin-like), transmembrane	**6.0**
	41372	Calcium-binding EF-hand (calmodulin-like)	−2.8
	42194	Calcium-binding EF-hand (calmodulin-like)	−2.4
	10164	Calcium-binding domain and potential peptidase domain	−4.3
	25392	Calcium-binding domain and potential peptidase domain, transmembrane	−2.4
	7230	Calcium-binding domain, regucalin	−3.3
	8014	Calcium-binding GLA (gamma-carboxyglutamic acid-rich) domain	−4.5
Ion channels and	711	Bile acid:Na symporter, transmembrane	−4.8
oxidative burst	3092	K+ inward voltage channel, transmembrane	**2.7**
	4725	Na/H antiporter, transmembrane	−10.5
	11375	NADPH oxidase/ferric reductase, transmembrane	**2.5**
Mitogen-activated protein	9710	MAPK	−8.8
kinase (MAPK) pathway	574	1-Deoxy-D-xylulose-5-phosphate synthase (dxs)	−2.2
terpenoid and	2376	Mevalonate kinase (MVK)	−2.1
carotenoid biosynthesis	6524	15-cis-phytoene desaturase (crtP)	−4.5
	10943	1-Deoxy-D-xylulose-5-phosphate reductoisomerase (dxr)	−3.6

Table 1. *cont.*

General function	Locus tag	Description	Fold change
	29228	(E)-4-Hydroxy-3-methylbut-2-enyl-diphosphate synthase (ispG)	−2.8
Protein phosphatases	31862	PP2C	**2.8**
2C-type (PP2Cs)	36303	PP2C	**2.2**
	37710	PP2C	**2.2**
	264143	PP2C	−2.5
Related signaling and	17208	Casein kinase II (CK2), beta subunit	**2.0**
regulatory proteins	23331	RAP (RNA-binding)- and FAST (Fas-activated serine/ threonine)-kinase-domain protein	−2.8
	23490	MHCK/EF2 (myosin heavy chain kinase/elongation factor-2) kinase	−4.1
	264261	Serine/threonine protein kinase and signal transduction histidine kinase	**6.0**
	33287	Ubiquitin-activating enzyme E1	**3.2**
	34838	Ubiquitin-conjugating enzyme E2	**2.8**
	10006	Ubiquitin hydrolase	**2.5**
	21460	Ubiquitin hydrolase	−2.4
	23994	Ubiquitin hydrolase	−4.3
	24982	Integrin, transmembrane	**5.0**
	3202	Fibronectin-binding protein	−6.3
	7648	Tumor necrosis factor receptor (TNFR)-associated factor 3 (TRAF3)	−4.8
	12050	Auxin efflux, transmembrane	−3.7
	25698	Interferon regulator	**2.2**
	24575	Guanylate cyclase	**3.1**
Endo- and exo-cytosis	1311	Epsin N-terminal	**2.4**
	2467	SNARE/syntaxin, transmembrane	**2.1**
	36490	Clathrin adaptor complex AP2 small chain	**2.4**
Cell cycle	11138	Cyclin-A-like, G2/mitotic-specfic cyclin	**4.6**
	25048	Cyclin-F-like, F-box domain	**9.5**
	36441	Cyclin-A-like, G2/mitotic-specfic cyclin	−4.1
	33772	Serine/threonine-protein kinase TTK/MPS1-like	−4.2
	9963	Regulator of chromosome condensation (RCC1)	−4.8
	38047	Regulator of chromosome condensation (RCC1)	**3.0**
	24000	c-myc promoter binding protein	**2.7**
	11019	Notch-like protein with EGF domains, transmembrane	**2.8**
	11191	Epidermal growth factor (EGF) domain	**2.9**
	2505	CASP1, metacaspase	**3.3**
	40348	cdc48, ATPase	−4.0
	40725	cdc48–2, ATPase	−3.4
	4020	Pirin	**2.2**
Chitin degradation and	24204	Chitinase	**3.5**
chitin-binding proteins	262153	Chitinase	**11.8**
	263782	Chitinase	**7.6**
	261895	Chitinase	**3.6**
	25905	Glycosyltransferase, putative	**2.4**
	36631	UDP-*N*-acetylglucosamine pyrophosphorylase (UAP1)	**4.3**
	37041	*N*-acetylgalactosamine-6-phosphate deacetylase (nagA)	**3.7**
	260958	Phosphoacetylglucosamine mutase	**6.1**
	22908	Chitin-binding domain protein	**3.2**
	25842	Chitin-binding domain protein	**4.3**
	262644	Chitin-binding domain protein	**3.1**
	268516	Chitin-binding domain protein	**10.6**
Upregulated transport	2088	Putative UDP-*N*-acetylglucosamine transporter	**2.4**
	11697	CBA1, cobalamin acquisition protein 1	**11.0**
	16722	ABC transporter, subfamily A, lipid transport	**3.3**
	26635	Amino acid/polyamine transporter	**2.2**
	38157	GDP-L-fucose transporter, presumed from cytosol to ER-Golgi lumen	**2.5**
	262236	Amino acid transporter, possibly cationic	**2.5**

Only those genes with $\geq$ twofold differential expression and an fdr <0.05 are shown (baySeq; Hardcastle and Kelly, 2010). Functional information is derived from Interpro, GO, Pfam and user annotations available for the *T. pseudonana* genome in the JGI Genome Portal. See Supporting Information Table S2 for a complete list of differentially expressed genes.

Table 2. Selected list of upregulated genes in *Ruegeria pomeroyi* DSS-3 (39 out of 101) highlighting those involved in organic matter acquisition when co-cultured with diatom *Thalassiosira pseudonana* ($n = 4$) relative to no-substrate controls ($n = 2$) after 8 h of growth.

General function	Locus tag	Description	Fold change
2,3-dihydroxypropane-1-sulfonate (DHPS) transport and catabolism	SPO0591	DHPS TRAP dicarboxylate transporter, DctP subunit (hpsK)	120.4
	SPO0592	DHPS TRAP dicarboxylate transporter, DctQ subunit (hpsL)	79.3
	SPO0593	DHPS TRAP dicarboxylate transporter, DctM subunit (hpsM)	126.0
	SPO0594	DHPS-3-dehydrogenase (hpsN)	79.5
	SPO0595	R or S-DHPS-2-dehydrogenase (hpsO)	373.5
	SPO0596	S or R-DHPS-2-dehydrogenase (hpsP)	131.2
	SPO0597	UspA universal stress family protein (hpsQ)	56.3
	SPO0598	Membrane-bound sulfolactate dehydrogenase (slcD)	193.0
	SPOA0157	Bisulfite exporter (cuyZ)	156.0
	SPOA0158	L-cysteate sulfo-lyase (cuyA)	71.2
N-*acetyltaurine (NAT) transport and catabolism*	SPO0658	NAT amidohydrolase (naaS)	14.0
	SPO0660	NAT ABC transporter, periplasmic peptide-binding protein (naaA)	30.2
	SPO0661	NAT ABC transporter, permease protein (naaB)	22.5
	SPO0662	NAT ABC transporter, permease protein (naaB')	24.0
	SPO0663	NAT ABC transporter, ATP-binding protein (naaC)	32.0
	SPO0664	NAT ABC transporter, ATP-binding protein (naaC')	4.5
Potential amide/urea transport and catabolism	SPO3659	LamB/YcsF family protein	17.1
	SPO3661	Allophanate hydrolase subunit 1	14.3
	SPO3662	Membrane protein	120.0
	SPO3664	TRAP dicarboxylate transporter, subunit DctQ subunit	16.5
	SPO3665	TRAP dicarboxylate transporter, periplasmic DctP subunit	11.0
Potential acidic sugar transport and catabolism	SPO2409	Oxidoreductase, putative 3-oxoacyl-ACP reductase	7.0
	SPO2410	Dihydroxy-acid dehydratase, putative xylonate dehydratase	6.2
	SPO2430	Altronate hydrolase UxaA/galactarate dehydratase	10.2
	SPO2433	TRAP dicarboxylate transporter, periplasmic DctP subunit, putative	6.4
Potential amino acid and/or osmolyte transport	SPO1018	Branched-chain amino acid ABC transporter, ATP-binding protein	6.3
	SPO2442	Glycine betaine/proline ABC transporter, permease protein	11.9
	SPO2443	Glycine betaine/proline ABC transporter, ATP-binding protein	33.0
	SPO2658	Glutamate/aspartate ABC transporter, periplasmic substrate-binding protein	44.6
	SPO2659	Glutamate/aspartate ABC transporter, permease protein	24.8
	SPO2660	Glutamate/aspartate ABC transporter, permease protein	17.0
	SPO2661	Glutamate/aspartate ABC transporter, ATP-binding protein	29.0
	SPO3705	Branched-chain amino acid ABC transporter, periplasmic binding protein	14.8
	SPO3708	Branched-chain amino acid ABC transporter, permease protein	18.0
Unidentified transport	SPO1111	Hypothetical protein	69.5
	SPO1112	TRAP transporter, periplasmic DctP subunit	67.7
	SPO1113	TRAP transporter, transmembrane DctQ subunit, putative	46.7
	SPO1114	TRAP transporter, transmembrane DctM subunit	24.8
	SPO1115	Hypothetical protein	16.7

Only those genes with $\geq$ twofold differential expression and an fdr <0.05 were included (baySeq; Hardcastle and Kelly, 2010). Functional information was derived from annotations available at Roseobase (www.roseobase.org). See Supporting Information Table S4 for a complete list of differentially expressed genes.

responses 8 h after inoculation identified 101 genes differentially regulated by *R. pomeroyi* in co-culture with *T. pseudonana* compared to the control (67 upregulated and 34 downregulated; Supporting Information Table S4).

Among the upregulated bacterial genes in the co-cultures were 24 annotated components of transporters that target organic compounds, including five multiprotein ABC transporter systems (ATP-binding cassette) and four TRAP transporter systems (tripartite ATP-independent periplasmic) (Table 2). One TRAP system mediates the uptake of the DHPS and one ABC system mediates *N*-acetyltaurine transport (Durham *et al*., 2015); genes encoding transport and metabolism of these sulfonates were only recently discovered (Mayer *et al*., 2010; Denger *et al*., 2011). Upregulation of nine metabolic genes mediating downstream catabolism of these sulfonates was also observed (Table 2). The substrates of the remaining upregulated transporters have not been experimentally verified. Four ABC transporters have general annotations for uptake of amino acids (glutamate/aspartate, branched-chain amino acids) and nitrogen-containing osmolytes (glycine betaine/proline), compounds that could also fulfill the nitrogen requirement of *R. pomeroyi* which is unable to use the nitrate supplied in the medium (Supporting Information Fig. S1). One of the TRAP transporters was adjacent to an upregulated gene annotated as an

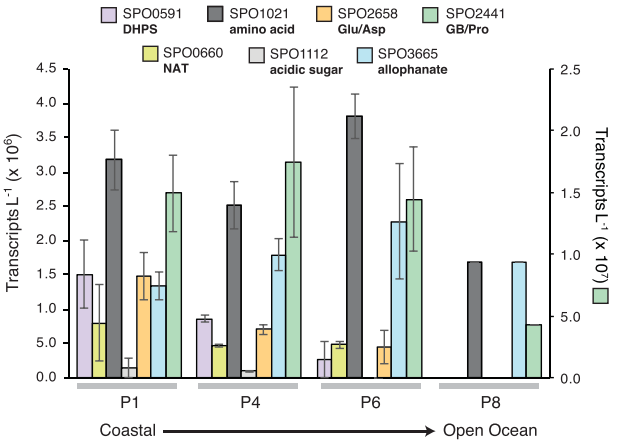

Fig. 3. Abundance of transcripts with sequence similarity to upregulated *R. pomeroyi* transporter systems (≥50% identity over ≥50% of read length) at four surface waters stations along the Line P transect in the eastern North Pacific in May 2013.
Error bars indicate the standard deviation of duplicate samples.
SPO0591, DHPS transport; SPO0660, *N*-acetyltaurine transport; SPO1021, possible branched-chain amino acid transport; SPO1112, Possible sugar transport; SPO2658, possible glutamate or aspartate transport; SPO3665, possible allophanate transport; SPO2441, possible glycine betaine or proline transport.

allophanate (urea-1-carboxylate) hydrolase subunit (SPO3661; Table 2). Since bacterial TRAP systems are often co-located with the gene encoding the first metabolic transformation of the transported compound (Mulligan *et al.*, 2011), allophanate is a possible substrate of this transporter. Another upregulated TRAP transporter gene was co-located with an upregulated gene annotated as a hydrolase/dehydratase of the sugar acid altronate or galactarate (SPO2430; Table 2).

Evidence for bacterial transporter expression in the surface ocean

Metatranscriptome data collected at four stations along the Line P transect during a diatom bloom in the eastern North Pacific in May 2012 was searched for orthologues to the upregulated *R. pomeroyi* transporters. This diatom bloom was dominated by a *Pseudo-nitzschia* species, with Roseobacter clade members accounting for 21%–85% of the bacterial community mRNA. Using substrate-binding transport proteins as query sequences, transcripts from potential orthologues were found for seven of the nine upregulated *R. pomeroyi* systems (Fig. 3). Four had a primarily coastal pattern: the DHPS transporter (SPO0591), the *N*-acetyltaurine transporter (SPO0660), the putative glutamate/aspartate transporter (SPO2658) and the putative sugar transporter (SPO1112). Three retained substantial expression out to the open ocean station: the putative branched-chain amino acid transporter (SPO1021), the possible allophanate transporter (SPO3665), and with ~10-fold higher abundance per liter of seawater than the others, the putative glycine betaine/proline transporter (SPO2441) (Fig. 3). Of these, two are transporters of organic sulphur compounds and five are transporters of known or predicted organic nitrogen compounds. There was no evidence that the bacterioplankton community was expressing the putative galactarate transporter (SPO2433) or the second branched-chain amino acid transporter (SPO3705).

Metabolomic response

At the same stages of culture development analysed for transcriptome analysis (8 h for the bacterium, 56 h for the diatom; Fig. 1), a suite of 78 metabolites representing a range of central and secondary metabolic pathways were measured. The diatom intracellular metabolites homocysteate and gluconate were significantly depleted in co-cultured *T. pseudonana* compared with the B_{12}-replete axenic control ($p < 0.05$). No diatom metabolites were significantly enriched during co-culture (Fig. 4).

Thirteen intracellular metabolites were significantly enriched ($p < 0.05$) in co-cultured *R. pomeroyi* cells compared with the mono-culture control in *f*/2 seawater medium (Fig. 4), and none were significantly depleted. Two sulfonate degradation pathway intermediates, sulfolactate and nitrogen-containing L-cysteate, were enriched 574- and 442-fold in co-cultured bacterial cells ($p < 0.001$). These represent the largest changes observed in the bacterial metabolome (Fig. 4). Also enriched was the amino acid phenylalanine (twofold, $p < 0.05$). Chitin monomers *N*-acetyl-glucosamine-1/6-phosphate (GlcNAc-1/6-P) and UDP-*N*-acetylglucosamine (UDP-GlcNAc) were both present in higher concentrations (twofold and threefold, respectively, although not significantly) in the *R. pomeroyi* metabolome (Fig. 4), potentially consistent with the differentially regulated chitin metabolism genes and transporter components in the diatom transcriptome. Finally, significant depletion of gluconate in the diatom metabolome was matched with a significant enrichment in the bacterial metabolome ($p < 0.05$) (Fig. 4). Gluconate is an intermediate in the Entner-Doudoroff pathway, the pathway *R. pomeroyi* uses for carbohydrate metabolism (Moran *et al.*, 2007).

Discussion

Currencies of microbial interactions may represent sizeable fluxes in the carbon cycle, yet they have been difficult to identify because of low steady state concentrations in bulk seawater and the challenges of novel compound identification (Moran *et al.*, 2016). In desert soil, for example, 80 different metabolites were found to be exchanged between bacterial cells yet most could not be chemically

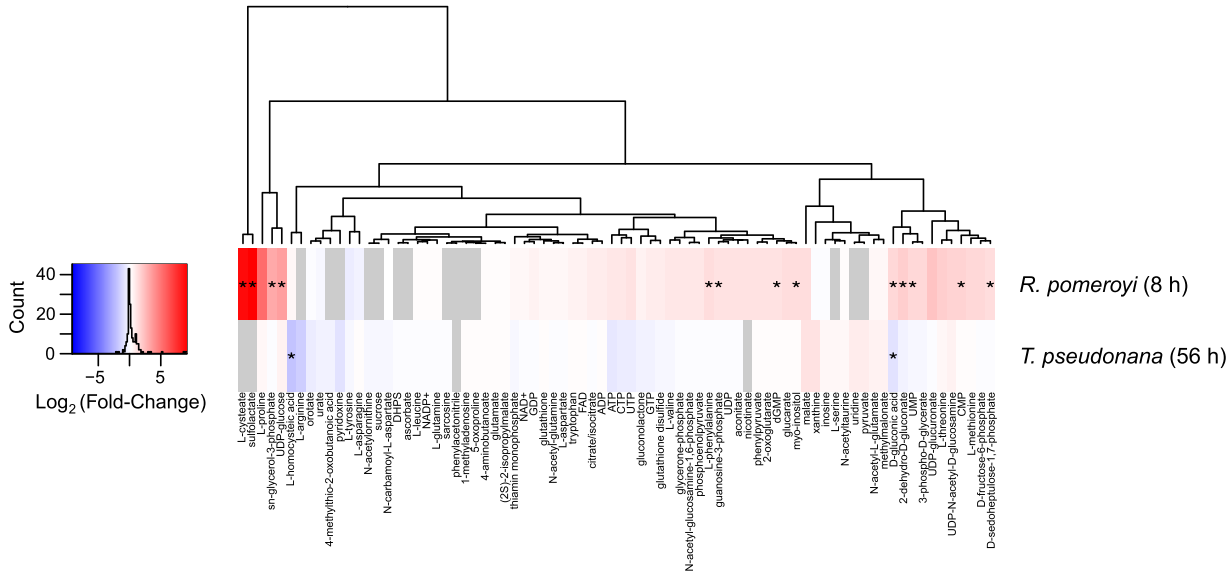

Fig. 4. Log_2-fold changes in intracellular metabolites in *Ruegeria pomeroyi* DSS-3 and *Thalassiosira pseudonana* in co-culture relative to controls.
Bacterial metabolite data are derived from the 8 h time point and diatom metabolite data are from the 56 h time point, representing the first time point for each with substantial differences in expression between mono- and co-cultures. Diatom and bacterial cells were separated by differential filtration, and data were corrected for cells in the incorrect size fraction based on flow cytometric analysis. Asterisks denote statistical significance at $p < 0.05$. Left: Log_2-fold-change color code and metabolite counts by fold-change bin. Grey = metabolite not detected.

identified (Baran *et al.*, 2015). Here, we took advantage of the ability of microbes to sensitively detect chemicals in their environment, using upregulation of transporter systems and metabolome shifts to single out specific metabolites potentially important in trophic interactions.

Substrates of two of the transporter systems upregulated by *R. pomeroyi* in co-culture with *T. pseudonana* were identified previously as sulfonates DHPS and *N*-acetyltaurine (Durham *et al.*, 2015). Other upregulated transporters point to metabolites whose roles in surface ocean heterotrophy have been recognized previously, such as amino acids and osmolytes (Wright and Hobbie, 1966; King, 1988; Kiene and Walker, 1998; Cottrell and Kirchman, 2000). Potential metabolites also include homocysteate, an unidentified acidic sugar and an unidentified amide, and these may represent novel metabolites participating in the transfer of recently fixed carbon to heterotrophic marine bacteria. Orthologues of the suite of upregulated transporters are expressed in the surface ocean, albeit to varying extents (Fig. 3).

The induction by bacteria of a putative diatom signal cascade was the most pervasive transcriptional response observed in the co-culture. This response involved differential expression of genes homologous to LRR receptors, secondary messengers, protein kinase systems and cell cycle regulators, among others (Table 1). LRR receptors are involved in protein-protein interactions in many organisms. In land plants, they have roles in immunity and developmental signaling by binding target ligands and relaying information on biotic and abiotic stimuli through the downstream response components of the CDPK and MAPK signal cascades (Felix *et al.*, 1999; Ligterink and Hirt, 2001; Diévart and Clark, 2004; Pitzschke *et al.*, 2009; Gao *et al.*, 2014). Close homologs of the three upregulated *T. pseudonana* LRR genes are present in six other *Thalassiosira* species (*T. oceanica*, *T. weissflogii*, *T. punctigera*, *T. gravida*, *T. antarctica* and *T. rotula*), several *Skeletoma* species, *Cyclotella meneghiniana* and *Detonula confervacea* (Supporting Information Figs. S2–4). More distant homologs were found in plants, bacteria, oomycetes and green algae, with identities of 26%–43% similarity to predicted LRR domains (Supporting Information Table S3). A search for sequences matching the diatom LRR proteins in the metatranscriptome of a *Pseudo-nitzschia* bloom in the North Pacific yielded no potential orthologues, although this is consistent with finding LRR homologs in the genomes of centric diatoms (which includes *Thalassiosira*) but not pennate diatoms (which includes *Pseudo-nitzschia*) (Supporting Information Table S3).

The differential expression of nine genes annotated as CDPKs or calcium-binding proteins (three upregulated, six downregulated) suggests similarities with plant recognition of bacteria using Ca^{2+} as a second messenger (Zimmermann *et al.*, 1997; Vadassery and Oelmüller, 2009). Calcium-dependent signaling followed by cell death was described previously for nutrient-limited diatoms (Vardi *et al.*, 2006), and our results extend this by suggesting the second messenger also plays a role in relaying information

on biotic stimuli. In the opportunistic pathogen *Pseudomonas aeruginosa*, calcium levels in mammalian host cells are modified by autoinducer signaling (Shiner *et al.*, 2006). The evidence of calcium-dependent signaling, together with differential regulation of three ion channels and an NADPH oxidase, indicative of ion flux and oxidative burst, respectively, implicate a suite of mechanisms used in the diatom which are typical of plant recognition systems (Jabs *et al.*, 1997; Lipinski *et al.*, 2009; Dubiella *et al.*, 2013). One metacaspase gene was upregulated, but although these proteins can play a role in programmed cell death in plants and fungi, this specific gene is thought to have a housekeeping role in *T. pseudonana* (Bidle and Bender, 2008).

In addition to a possible signaling cascade, another prevalent diatom transcriptional signal involved differential regulation of a suite of genes encoding chitin binding and chitin metabolism (Table 1). Diatoms synthesize chitin as part of their cell wall (Durkin *et al.*, 2009), and marine bacteria have been shown to target chitinous regions of diatom cells for attachment (Frischkorn *et al.*, 2013; Li *et al.*, 2016). Chitin monomers such as *N*-acetylglucosamine (GlcNAc) can also regulate bacterial virulence factors (Konopka, 2012) as well as serve as bacterial substrates (Wiegmann *et al.*, 2014). Indeed, we detected enrichment (though not significant) of chitin monomers GlcNAc-1/6-P and UDP-GlcNAc in the *R. pomeroyi* metabolome (Fig. 4). The diatom transcriptional response also involved urea cycle gene *unCPS*, which mediates the conversion of ammonium and bicarbonate to carbamoyl phosphate. Its downregulation may signal availability of ammonium derived from bacterial regeneration, as this gene has been shown previously to be involved in managing the nitrogen status of diatom cells (Allen *et al.*, 2011).

Previous studies of another Roseobacter in co-culture with a coccolithophore suggested that pathogenic attack was initiated when the bacterium detected senescence signals from the phytoplankton (Seyedsayamdost *et al.*, 2011; Segev *et al.*, 2016). However, no observed differences in the physiological state of *T. pseudonana* (i.e., growth rate, photosynthetic parameter F_v/F_m) were observed between mono- and co-culture conditions in this study, and transfer of cells into fresh medium reinitiated exponential growth for both treatments (Supporting Information Fig. S5). Further, upregulation of the diatom's cobalamin acquisition protein CBA1 and the bacterium's organic compound transporters are not suggestive of pathogenic interactions. However, we noticed that diatoms in stationary phase cultures decreased in both cell number (Fig. 1) and chlorophyll *a* content more quickly in the presence of the bacterium, and there was also evidence of increased bacterial attachment to diatom cells in stationary phase (up to 10 per diatom cell) relative to exponential phase. These observations might argue for the onset of a pathogenic stage as the co-culture senesced, or could signify efficient recycling of cell detritus by the bacteria.

There are no known systems encoded in the *R. pomeroyi* genome that could mediate direct interactions with phytoplankton cells, although other members of the Roseobacter lineage have mechanisms such as Type IV and Type VI secretion systems (Moran *et al.*, 2007; Persson *et al.*, 2009; Newton *et al.*, 2010). Further, the low numbers of bacterial cells attached to diatoms during exponential growth suggest that diffusible chemicals are a more likely mechanism for regulating the putative diatom signal recognition proteins. Upregulated bacterial genes that could participate in the release of diffusible chemical signals include two genes of the Tat (twin-arginine translocation) system for protein export (SPO2681 and SPO2682) and a gene encoding a lipopolysaccharide exporter (SPO2454) (Supporting Information Table S4). Vitamin B_{12} could be considered a candidate for the chemical signal based on evidence of uptake by the diatom (Fig. 1), yet the lack of a diatom transcriptional response to exogenous B_{12} addition and no evidence of bacterial upregulation of B_{12} biosynthesis argues against this. Other known bacterial molecules that trigger recognition mechanisms in plants include flagellin, lipopolysaccharides, siderophores and acylhomoserine lactones (Diévart and Clark, 2004; Meziane *et al.*, 2005; Schuhegger *et al.*, 2006; Yue *et al.*, 2012).

Two hypotheses emerged from this transcriptomic and metabolomic analysis of a bacteria-diatom co-culture. First, bacterial secondary production was supported by substrates dominated by organic nitrogen and organic sulphur compounds. Second, *R. pomeroyi–T. pseudonana* interactions may extend beyond passive release and uptake of metabolites to include a potential diatom recognition system for the presence of the bacterium. The microbes selected for this model system represent two abundant lineages of marine plankton. Further, they commonly co-occur in the ocean, are capable of blooming to high numbers, and are proposed to have a shared evolutionary history (Pinhassi *et al.*, 2004; Grossart *et al.*, 2005; Amin *et al.*, 2012; Luo *et al.*, 2013). Such interdependencies between natural populations of bacteria and phytoplankton may have important influences over both rates and timing of carbon transformations in the ocean.

Experimental procedures

Co-culture experimental setup

R. pomeroyi DSS-3 was streaked to isolation on ½ YTSS agar, after which single colonies were inoculated into liquid ½ YTSS and grown overnight at 30°C in the dark at 200 r.p.m. Cells were harvested in exponential phase, washed twice in *f*/2 medium (+Si, –B_{12}) (Guillard, 1975) and resuspended in *f*/2 (+Si, –B_{12}) to ~1×10^8 cells mL^{-1}. This inoculum was diluted 1:100 when added to the co-culture. *T. pseudonana* CCMP1335 was cultured in *f*/2 medium (+Si) in a diurnal

incubator at 18°C on a 16:8 h light:dark cycle at ~160 μmol photons m^{-2} sec^{-1}. The diatom was limited for vitamin B_{12} over three sequential transfers into *f*/2 without B_{12} (+Si, $-B_{12}$) at which point cell growth rate decreased significantly (~50%) as compared with cells grown in *f*/2 with B_{12}. The B_{12}-limited *T. pseudonana* culture was diluted to ~10^4 cells mL^{-1} in fresh *f*/2 (+Si, $-B_{12}$) at the start of the experiment.

Four treatments ($n = 3$–4 replicates for each) were established as follows: (1) *T. pseudonana* + B_{12} (370 pM cyanocobalamin), (2) *T. pseudonana* (no B_{12} addition), (3) *T. pseudonana* + *R. pomeroyi* (no B_{12} addition) and (4) *R. pomeroyi* alone (no B_{12} addition), as previously described (Durham *et al.*, 2015). Treatments 1 and 3 were compared for differences in diatom gene expression and intracellular metabolite pools in the presence versus absence of the bacterium. Treatments 3 and 4 were compared for differences in bacterial gene expression and intracellular metabolite pools in the presence and absence of the diatom. Because the *f*/2 medium contained no organic compounds, bacterial growth was dependent solely on phytoplankton-derived molecules; thus, there was no change in cell abundance in Treatment 4 (Fig. 1, Supporting Information Fig. S1).

Diatom and bacterial abundance during the experiment was tracked with a Beckman Coulter CyAn flow cytometer. Samples were stained with SYBR-Green II (Molecular Probes/Invitrogen, Carlsbad, CA, USA), and diatom and bacterial cells were enumerated using a combination of side-scatter and red and green fluorescence, respectively, with comparison to known concentrations of fluorescent beads (Fluoresbrite TG Carboxylate 1.75 μm Microspheres; Polysciences Inc.). Changes in diatom abundance were also tracked using relative fluorescent units of chlorophyll *a* on a BioTek Synergy Mx microplate reader. Axenic diatom cultures were checked for bacterial contamination during the flow cytometry analysis and were also routinely analysed by epifluorescence microscopy using DAPI (4′,6-diamidino-2-phenylindole) staining and by spread plating on ½ YTSS agar. Treatments 1 and 2 remained axenic throughout the experiment.

Transcriptome analyses

From replicate cultures ($n = 2$ or $n = 4$) in each treatment, cells were collected for RNA extraction at the midpoint of the light cycle at two times: 8 h after initiation of the co-culture for both bacteria and diatoms and during the exponential phase of growth for diatoms (at 56 h; Fig. 1). Cultures were filtered onto 0.2 μm membrane filters, and filters were flash-frozen in liquid N_2 and subsequently stored at −80°C. Bacterial transcriptomes and poly(A)-selected diatom transcriptomes were prepared as previously described (Durham *et al.*, 2015), and sequenced on Illumina MiSeq (Illumina Inc., San Diego, CA) or SOLiD version 4 (Life Technologies, New York) sequencing platforms. Sequence data are available in the NCBI BioProject database (accession number PRJNA261079).

Reads were mapped to the genomes of *R. pomeroyi* DSS-3 (www.roseobase.org) and *T. pseudonana* (Thaps3 FilteredModels2 from the Joint Genome Institute portal) using BWA (v.0.5.9) (Li and Durbin, 2009). The number of *R. pomeroyi* and *T. pseudonana* sequence reads that aligned to gene models were calculated from the resulting SAM alignment files, and only sequences aligning to gene models were used for subsequent analyses. Mapped read counts were analysed for significant differential expression using the baySeq package in R (Hardcastle and Kelly, 2010) with fdr < 0.05 as the significance cut-offs. For the diatom transcriptomes, a two-way comparison was performed on axenic ($n = 2$, Treatment 1) versus bacterized ($n = 2$, Treatment 3) biological replicates; for the bacterial transcriptomes, a two-way comparison was performed on biological replicates with diatoms ($n = 4$, Treatment 3) versus without diatoms ($n = 2$, Treatment 4).

For phylogenetic tree construction, full-length protein sequences of *T. pseudonana* LRR domain-containing proteins Tp5595, Tp20707 and Tp25675 were used as queries to identify putative orthologues in marine microeukaryote transcriptome assemblies from the Marine Microbial Eukaryote Transcriptome Sequencing Project (MMETSP; http://marinemicroeukaryotes.org) (Keeling *et al.*, 2014) available from iMicrobe using BLASTp (e-value cutoff 1e-05). Potential orthologue sequences were aligned using MAFFT (Katoh and Standley, 2013) with the E-ISN-i algorithm. The resulting alignment regions were trimmed using trimAl (Capella-Gutiérrez *et al.*, 2009), and alignment files were converted to Phylip format. The best-fit amino acid substitution matrix and among-site rate heterogeneity model were determined using the ProtTest software (Abascal *et al.*, 2005). Outgroups included related LRR-domain-containing proteins in *T. pseudonana*.

Metatranscriptomic data from plankton at GeoMICS project Line P stations P1, P4, P6, P8 were obtained using the same methods as for the laboratory cultures as described above with two exceptions. First, bacterioplankton cells were collected by filtration through a 0.2 μm pore-size filter (142 mm diameter Supor) following prefiltration through a 2.0 μm pore-size filter (142 mm diameter polycarbonate). Second, two internal standards ~1,000 nt in length were added independently to the lysis buffer in known copy numbers so that absolute transcript values could be calculated per liter of sample filtered (Satinsky *et al.*, 2013). cDNAs were sheared ultrasonically to ~250 base pair fragments and HiSeq libraries (Illumina Inc., San Diego, CA) were constructed for paired-end (2 × 150) sequencing using the Illumina HiSeq 2500 sequencing platform (Illumina Inc., San Diego, CA). Reads were joined using PANDAseq (Masella *et al.*, 2012) and paired reads were trimmed using FASTX-Toolkit (http://hannonlab.cshl.edu/fastx_toolkit/). rRNA, tRNA and internal standard sequences were removed using a BLASTn search against a database containing representative rRNA and tRNA sequences along with the internal standard sequence (bit score cutoff ≥50). Protein sequences of the upregulated *R. pomeroyi* transporters (using substrate binding protein for TRAP and ABC transporters) were used as query sequences in a BLASTx search of the GeoMICS reads. Alignment with the query sequence for at least 50% of read length with at least 50% identity were the criteria used to identify positive hits. Transcript concentration in seawater was calculated based on recovery of the internal standard reads. Sequence data are available in the NCBI BioProject database (accession number PRJNA272345).

Metabolite analysis

Intracellular metabolites were collected from the cultures at the time of transcriptome sampling (8 h for the bacteria, $n = 3$,

and 56 h for the diatom, $n = 3$). Cells from 100 mL of culture were collected and processed by sequential filtration onto 3.0 μm (mostly diatom cells) and 0.2 μm (mostly bacterial cells) filters. Filters were flash frozen in liquid N_2 and stored at −80°C. Metabolites were analysed as in Durham and colleagues (2015) by ultra-performance liquid chromatography-high resolution mass spectrometry (UPLC-HRMS). Briefly, frozen samples were suspended in HPLC grade methanol at 4°C for extraction. Following centrifugation, two additional pellet extractions were carried out in 80% methanol in water at 4°C. Combined supernatants from the consecutive methanol extractions were dried under N_2 and solid residue was resuspended in sterile water at 4°C. A 10-μL aliquot was injected through a Synergi 2.5 μm Hydro-RP 100, 100 × 2.00 mm LC column (Phenomenex) kept at 25°C. The mass spectrometer was run in full scan mode with negative ionization using a method adapted from Rabinowitz and Kimball (2007). The eluent was introduced into the MS via an electrospray ionization source conjoined to a Thermo Scientific Exactive Plus orbitrap mass spectrometer through a 0.1 mm internal diameter fused silica capillary tube. The samples were run with a spray voltage of 3 kV. The nitrogen sheath gas was set to a flow rate of 10 psi with a capillary temperature of 320°C and an Automatic Gain Control target set to $3x10^6$. Samples were analysed with a resolution of 140,000 at 200 *m*/*z* and a scan window of 85 to 800 *m*/*z* from 0 to 9 min and 110 to 1000 *m*/*z* from 9 to 25 min. The chromatography gradient consisted of an initial hold of 100% solvent A (97:3 water:methanol, 10 mM tributylamine and 15 mM acetic acid 0.1% formic acid in water) and 0% B (methanol) for 5 min, ramp to 20% B from 5 to 13 min, ramp to 55% B from 13 to 15.5 min, ramp to 85% B from 15.5 to 19 min and ramp to 0% B from 19–25 min, with a flow rate of 200 μL min^{-1}. Seventy-eight known metabolites based on pure standards were manually selected by mass (± 5 p.p.m.) and retention time.

Per-cell ion current values for each metabolite were calculated based on background-subtracted total ions and cell count values. Flow-cytometry-based cell counts were used to determine the number of bacteria and diatoms in each size fraction after sequential filtration of the co-cultures. The ion contribution of contaminating cells was subtracted from the metabolite measurements based on analysis of per-cell metabolite concentrations in axenic cultures of the contaminating organism. An average of 20% of the bacterial cells were caught on the 3.0 μm filters and an average of 0.5% of the diatom cells were caught on the 0.2 μm filters. Statistical significance was based on the Student's *t*-test. A heatmap was generated using the gplots package in R (Warnes *et al*., 2015) with $p < 0.05$ significance denoted. Identification of significantly different metabolites was similar regardless of whether or not contributions of contaminating cells were subtracted.

Growth requirements of R. pomeroyi

To determine the ability of select organic compounds to satisfy *R. pomeroyi* carbon and nitrogen requirements, the bacterium was grown in *f*/2 medium (+Si, $-B_{12}$) with either dihydroxypropanesulfonate (DHPS), *N*-acetyltaurine or acetate serving as carbon sources at equimolar concentrations (10 mM) and either urea or ammonium serving as nitrogen sources at equimolar concentrations (5 mM).

Acknowledgements

We appreciate the advice and assistance of B. Hopkinson, B. Satinsky, L. Chan, N. Lawler, C. English, C. Berthiaume, R. Morales, M. Parker, R. Nilson, B. Kvitko and S. Smith. This research was partially funded by the Gordon and Betty Moore Foundation grants 538.01 to M.A.M. and 537.01 to E.V.A., and by NSF grants OCE-1356010 to M.A.M. and OCE-1205233 to E.V.A. Resources and technical expertise were provided by the University of Georgia's Georgia Advanced Computing Resource Center. Conflict of interest statement: The authors declare that there are no conflicts of interest.

References

Abascal, F., Zardoya, R., and Posada, D. (2005) ProtTest: selection of best-fit models of protein evolution. *Bioinformatics* **21:** 2104–2105.

Aharonovich, D., and Sher, D. (2016) Transcriptional response of *Prochlorococcus* to co-culture with a marine *Alteromonas*: differences between strains and the involvement of putative infochemicals. *ISME J* **10:** 2892–2906.

Allen, A.E., Dupont, C.L., Oborník, M., Horák, A., Nunes-Nesi, A., McCrow, J.P., *et al*. (2011) Evolution and metabolic significance of the urea cycle in photosynthetic diatoms. *Nature* **473:** 203–207.

Amin, S.A., Hmelo, L.R., van Tol, H.M., Durham, B.P., Carlson, L.T., Heal, K.R., *et al*. (2015) Interaction and signalling between a cosmopolitan phytoplankton and associated bacteria. *Nature* **522:** 98–101.

Amin, S.A., Parker, M.S., and Armbrust, E.V. (2012) Interactions between diatoms and bacteria. *Microbiol Mol Biol Rev* **76:** 667–684.

Azam, F., and Malfatti, F. (2007) Microbial structuring of marine ecosystems. *Nat Rev Microbiol* **5:** 782–791.

Azam, F., Fenchel, T., Field, J., Gray, J., Meyer-Reil, L., and Thingstad, F. (1983) The ecological role of water column microbes in the sea. *Mar Ecol Prog Ser* **10:** 257–263.

Baran, R., Brodie, E.L., Mayberry-Lewis, J., Hummel, E., Da Rocha, U.N., Chakraborty, R., *et al*. (2015) Exometabolite niche partitioning among sympatric soil bacteria. *Nat. Commun* **6:** 8289.

Bell, W., and Mitchell, R. (1972) Chemotactic and growth responses of marine bacteria to algal extracellular products. *Biol Bull* **143:** 265–277.

Bertrand, E.M., Allen, A.E., Dupont, C.L., Norden-Krichmar, T.M., Bai, J., Valas, R.E., and Saito, M.A. (2012) Influence of cobalamin scarcity on diatom molecular physiology and identification of a cobalamin acquisition protein. *Proc Natl Acad Sci USA* **109:** E1762–E1771.

Bidle, K.D., and Bender, S.J. (2008) Iron starvation and culture age activate metacaspases and programmed cell death in the marine diatom *Thalassiosira pseudonana*. *Eukaryot Cell* **7:** 223–236.

Bidle, K.D., Manganelli, M., and Azam, F. (2002) Regulation of oceanic silicon and carbon preservation by temperature control on bacteria. *Science* **298:** 1980–1984.

Brand, L.E., and Guillard, R.R.L. (1981) A method for the rapid and precise determination of acclimated phytoplankton reproduction rates. *J Plankton Res* **3:** 193–201.

Capella-Gutiérrez, S., Silla-Martínez, J.M., and Gabaldón, T. (2009) trimAl: a tool for automated alignment trimming in large-scale phylogenetic analyses. *Bioinformatics* **25:** 1972–1973.

Cottrell, M.T., and Kirchman, D.L. (2000) Natural assemblages of marine Proteobacteria and members of the Cytophaga-Flavobacter Cluster consuming low- and high-molecular-weight dissolved organic matter. *Appl Environ Microbiol* **66:** 1692–1697.

Croft, M.T., Lawrence, A.D., Raux-Deery, E., Warren, M.J., and Smith, A.G. (2005) Algae acquire vitamin B12 through a symbiotic relationship with bacteria. *Nature* **438:** 90–93.

Danquah, A., de Zelicourt, A., Colcombet, J., and Hirt, H. (2014) The role of ABA and MAPK signaling pathways in plant abiotic stress responses. *Biotechnol Adv* **32:** 40–52.

Denger, K., Lehmann, S., and Cook, A.M. (2011) Molecular genetics and biochemistry of *N*-acetyltaurine degradation by *Cupriavidus necator* H16. *Microbiology* **157:** 2983–2991.

Diévart, A., and Clark, S.E. (2004) LRR-containing receptors regulating plant development and defense. *Development* **131:** 251–261.

Dubiella, U., Seybold, H., Durian, G., Komander, E., Lassig, R., Witte, C.-P., *et al*. (2013) Calcium-dependent protein kinase/NADPH oxidase activation circuit is required for rapid defense signal propagation. *Proc Natl Acad Sci USA* **110:** 8744–8749.

Durham, B.P., Sharma, S., Luo, H., Smith, C.B., Amin, S.A., Bender, S.J., *et al*. (2015) Cryptic carbon and sulfur cycling between surface ocean plankton. *Proc Natl Acad Sci USA* **112:** 453–457.

Durkin, C.A., Mock, T., and Armbrust, E.V. (2009) Chitin in diatoms and its association with the cell wall. *Eukaryot Cell* **8:** 1038–1050.

Felix, G., Duran, J.D., Volko, S., and Boller, T. (1999) Plants have a sensitive perception system for the most conserved domain of bacterial flagellin. *Plant J* **18:** 265–276.

Ford, M.G.J., Mills, I.G., Peter, B.J., Vallis, Y., Praefcke, G.J.K., Evans, P.R., and McMahon, H.T. (2002) Curvature of clathrin-coated pits driven by epsin. *Nature* **419:** 361–366.

Frischkorn, K.R., Stojanovski, A., and Paranjpye, R. (2013) *Vibrio parahaemolyticus* type IV pili mediate interactions with diatom-derived chitin and point to an unexplored mechanism of environmental persistence. *Environ Microbiol* **15:** 1416–1427.

Gao, X., Cox, K., Jr., and He, P. (2014) Functions of calcium-dependent protein kinases in plant innate immunity. *Plants* **3:** 160–176.

Gärdes, A., Iversen, M.H., Grossart, H.-P., Passow, U., and Ullrich, M.S. (2011) Diatom-associated bacteria are required for aggregation of *Thalassiosira weissflogii*. *ISME J* **5:** 436–445.

Geng, H., and Belas, R. (2010) Molecular mechanisms underlying roseobacter-phytoplankton symbioses. *Curr Opin Biotechnol* **21:** 332–338.

González, J.M., Simó, R., Massana, R., Covert, J.S., Casamayor, E.O., Pedrós-Alió, C., and Moran, M.A. (2000) Bacterial community structure associated with a dimethylsulfoniopropionate-producing North Atlantic algal bloom. *Appl Env Microbiol* **66:** 4237–4246.

Grossart, H.-P., Levold, F., Allgaier, M., Simon, M., and Brinkhoff, T. (2005) Marine diatom species harbour distinct bacterial communities. *Environ Microbiol* **7:** 860–873.

Guillard, R.R.L. (1975) Culture of phytoplankton for feeding marine invertebrates. In *Culture of Marine Invertebrate Animals*. Smith, W.L., and Chanley, M.H. (eds). New York, USA: Plenum Press, pp. 26–60.

Hardcastle, T.J., and Kelly, K.A. (2010) baySeq: empirical Bayesian methods for identifying differential expression in sequence count data. *BMC Bioinformatics* **11:** 422.

Helliwell, K.E., Wheeler, G.L., Leptos, K.C., Goldstein, R.E., and Smith, A.G. (2011) Insights into the evolution of vitamin B12 auxotrophy from sequenced algal genomes. *Mol Biol Evol* **28:** 2921–2933.

Hughes, D.T., and Sperandio, V. (2008) Inter-kingdom signalling: communication between bacteria and their hosts. *Nat Rev Microbiol* **6:** 111–120.

Jabs, T., Tschope, M., Colling, C., Hahlbrock, K., and Scheel, D. (1997) Elicitor-stimulated ion fluxes and O2- from the oxidative burst are essential components in triggering defense gene activation and phytoalexin synthesis in parsley. *Proc Natl Acad Sci USA* **94:** 4800–4805.

Katoh, K., and Standley, D.M. (2013) MAFFT multiple sequence alignment software version 7: improvements in performance and usability. *Mol Biol Evol* **30:** 772–780.

Keeling, P.J., Burki, F., Wilcox, H.M., Allam, B., Allen, E.E., Amaral-Zettler, L.A., *et al*. (2014) The Marine Microbial Eukaryote Transcriptome Sequencing Project (MMETSP): illuminating the functional diversity of eukaryotic life in the oceans through transcriptome sequencing. *PLoS Biol* **12:** e1001889.

Kerkhof, L.J., Voytek, M.A., Sherrell, R.M., Millie, D., and Schofield, O. (1999) Variability in bacterial community structure during upwelling in the coastal ocean. *Hydrobiologia* **401:** 139–148.

Kiene, R.P., and Walker, E. (1998) Seawater microorganisms have a high affinity glycine betaine uptake system which also recognizes dimethylsulfoniopropionate. *Aquat Microb Ecol* **15:** 39–51.

King, G.M. (1988) Distribution and metabolism of quaternary amines in marine sediments. In *Nitrogen Cycling in Coastal Marine Environments*. Blackburn, T., and Sorensen, J. (eds). New York, USA: Wiley, pp. 143–173.

Konopka, J.B. (2012) *N*-acetylglucosamine (GlcNAc) functions in cell signaling. *Scientifica* **2012:** 631–632.

Li, H., and Durbin, R. (2009) Fast and accurate short read alignment with Burrows-Wheeler transform. *Bioinformatics* **25:** 1754–1760.

Li, Y., Lei, X., Zhu, H., Zhang, H., Guan, C., Chen, Z., *et al*. (2016) Chitinase producing bacteria with direct algicidal activity on marine diatoms. *Sci Rep* **6:** 21984.

Ligterink, W., and Hirt, H. (2001) Mitogen-activated protein (MAP) kinase pathways in plants: versatile signaling tools. *Int Rev Cytol* **201:** 209–275.

Lipinski, S., Till, A., Sina, C., Arlt, A., Grasberger, H., Schreiber, S., and Rosenstiel, P. (2009) DUOX2-derived reactive oxygen species are effectors of NOD2-mediated antibacterial responses. *J Cell Sci* **122:** 3522–3530.

Luo, H., Csuros, M., Hughes, A.L., and Moran, M.A. (2013) Evolution of divergent life history strategies in marine Alphaproteobacteria. *MBio* **4:** e00373–e00313.

Manefield, M., Rasmussen, T.B., Henzter, M., Andersen, J.B., Steinberg, P., Kjelleberg, S., and Givskov, M. (2002) Halogenated furanones inhibit quorum sensing through accelerated LuxR turnover. *Microbiology* **148:** 1119–1127.

Masella, A.P., Bartram, A.K., Truszkowski, J.M., Brown, D.G., and Neufeld, J.D. (2012) PANDAseq: paired-end assembler for illumina sequences. *BMC Bioinformatics* **13:** 31.

Mayali, X., and Azam, F. (2004) Algicidal bacteria in the sea and their impact on algal blooms. *J Eukaryot Microbiol* **51:** 139–144.

Mayer, J., Huhn, T., Habeck, M., Denger, K., Hollemeyer, K., and Cook, A.M. (2010) 2,3-Dihydroxypropane-1-sulfonate degraded by *Cupriavidus pinatubonensis* JMP134: purification of dihydroxypropanesulfonate 3-dehydrogenase. *Microbiology* **156:** 1556–1564.

Mayers, T.J., Bramucci, A.R., Yakimovich, K.M., and Case, R.J. (2016) A bacterial pathogen displaying temperature-enhanced virulence of the microalga *Emiliania huxleyi*. *Front Microbiol* **7:** 892.

Meziane, H., Van Der Sluis, I., Van Loon L.C., Höfte, M., and Bakker, P.A. (2005) Determinants of *Psuedomonas putida* WCS358 involved in inducing systemic resistance in plants. *Mol Plant Path* **6:** 177–185.

Moran, M.A., Belas, R., Schell, M.A., González, J.M., Sun, F., Sun, S., *et al*. (2007) Ecological genomics of marine Roseobacters. *Appl Environ Microbiol* **73:** 4559–4569.

Moran, M.A., Kujawinski, E.B., Stubbins, A., Fatland, R., Aluwihare, L.I., Buchan, A., *et al*. (2016) Deciphering ocean carbon in a changing world. *Proc Natl Acad Sci USA* **113:** 3143–3151.

Mulligan, C., Fischer, M., and Thomas, G.H. (2011) Tripartite ATP-independent periplasmic (TRAP) transporters in bacteria and archaea. *FEMS Microbiol Rev* **35:** 68–86.

Nelson, D.M., Tréguer, P., Brzezinski, M.A., Leynaert, A., and Quéguiner, B. (1995) Production and dissolution of biogenic silica in the ocean: revised global estimates, comparison with regional data and relationship to biogenic sedimentation. *Glob Biogeochem Cycles* **9:** 359–372.

Newton, R.J., Griffin, L.E., Bowles, K.M., Meile, C., Gifford, S., Givens, C.E., *et al*. (2010) Genome characteristics of a generalist marine bacterial lineage. *ISME J* **4:** 784–798.

Obernosterer, I., and Herndl, G.J. (1995) Phytoplankton extracellular release and bacterial growth: dependence on the inorganic N:P ratio. *Mar Ecol Prog Ser* **116:** 247–258.

Paul, C., Mausz, M.A., and Pohnert, G. (2012) A co-culturing/metabolomics approach to investigate chemically mediated interactions of planktonic organisms reveals influence of bacteria on diatom metabolism. *Metabolomics* **9:** 349–359.

Persson, O.P., Pinhassi, J., Riemann, L., Marklund, B.-I., Rhen, M., Normark, S., González J.M., and Hagström, Å. (2009) High abundance of virulence gene homologues in marine bacteria. *Environ Microbiol* **11:** 1348–1357.

Pinhassi, J., Havskum, H., Peters, F., and Malits, A. (2004) Changes in bacterioplankton composition under different phytoplankton regimens. *Appl Environ Microbiol* **70:** 6753–6766.

Pitzschke, A., Schikora, A., and Hirt, H. (2009) MAPK cascade signalling networks in plant defence. *Curr Opin Plant Biol* **12:** 421–426.

Rabinowitz, J.D., and Kimball, E. (2007) Acidic acetonitrile for cellular metabolome extraction from Escherichia coli. *Anal Chem* **79:** 6167–6173.

Satinsky, B.M., Gifford, S.M., Crump, B.C., and Moran, M.A. (2013) Use of internal standards for quantitative metatranscriptome and metagenome analysis. In *Methods in Enzymology.* DeLong, E.F. (ed.). Elsevier Inc., Burlington, MA, Academic Press, pp. 237–250.

Schuhegger, R., Ihring, A., Gantner, S., Bahnweg, G., Knappe, C., Vogg, G., *et al*. (2006) Induction of systemic resistance in tomato by N-acyl-L-homoserine lactone-producing rhizosphere bacteria. *Plant Cell Environ* **29:** 909–918.

Schweighofer, A., Hirt, H., and Meskiene, I. (2004) Plant PP2C phosphatases: emerging functions in stress signaling. *Trends Plant Sci* **9:** 236–243.

Segev, E., Wyche, T.P., Kim, K.H., Petersen, J., Ellebrandt, C., Vlamakis, H., *et al*. (2016) Dynamic metabolic exchange governs a marine algal-bacterial interaction. *Elife* **5:** 514–522.

Seyedsayamdost, M.R., Case, R.J., Kolter, R., and Clardy, J. (2011) The Jekyll-and-Hyde chemistry of *Phaeobacter gallaeciensis*. *Nat Chem* **3:** 331–335.

Seyedsayamdost, M.R., Wang, R., Kolter, R., and Clardy, J. (2014) Hybrid biosynthesis of roseobacticides from algal and bacterial precursor molecules. *J Am Chem Soc* **136:** 15150–15153.

Shiner, E.K., Terentyev, D., Bryan, A., Sennoune, S., Martinez-Zaguilan, R., Li, G., *et al*. (2006) Pseudomonas aeruginosa autoinducer modulates host cell responses through calcium signalling. *Cell Microbiol* **8:** 1601–1610.

Suzuki, M.T., Béjà, O., Taylor, L.T., and DeLong, E.F. (2001) Phylogenetic analysis of ribosomal RNA operons from uncultivated coastal marine bacterioplankton. *Env Microbiol* **3:** 323–331.

van Tol, H.M., Amin, S.A., and Armbrust, E.V. (2017) Ubiquitous marine bacterium inhibits diatom cell division. *ISME J* **11:** 31–42.

Vadassery, J., and Oelmüller, R. (2009) Calcium signaling in pathogenic and beneficial plant microbe interactions: what can we learn from the interaction between *Piriformospora indica* and *Arabidopsis thaliana*. *Plant Signal Behav* **4:** 1024–1027.

Vardi, A., Formiggini, F., Casotti, R., De Martino, A., Ribalet, F., Miralto, A., and Bowler, C. (2006) A stress surveillance system based on calcium and nitric oxide in marine diatoms. *PLoS Biol* **4:** 0411–0419.

Wang, H., Tomasch, J., Jarek, M., and Wagner-Döbler, I. (2014) A dual-species co-cultivation system to study the interactions between Roseobacters and dinoflagellates. *Front Microbiol* **5:** 311.

Warnes, G.R., Bolker, B., Bonebakker, L., Gentleman, R., Liaw, W.H.A., Lumley, T., *et al*. (2015) gplots: various R Programming Tools for Plotting Data. *R Package version 2.17.0*.

Wiegmann, K., Hensler, M., Wöhlbrand, L., Ulbrich, M., Schomburg, D., and Rabus, R. (2014) Carbohydrate catabolism in *Phaeobacter inhibens* DSM 17395, a member of the marine roseobacter clade. *Appl Environ Microbiol* **80:** 4725–4737.

Wright, R.R., and Hobbie, J.E. (1966) Use of glucose and acetate by bacteria and algae in aquatic ecosystems. *Ecology* **47:** 447–464.

Xie, B., Bishop, S., Stessman, D., Wright, D., Spalding, M.H., and Halverson, L.J. (2013) *Chlamydomonas reinhardtii*

thermal tolerance enhancement mediated by a mutualistic interaction with vitamin B12-producing bacteria. *ISME J* **7:** 1544–1555.

Yue, J.-X., Meyers, B.C., Chen, J.-Q., Tian, D., and Yang, S. (2012) Tracing the origin and evolutionary history of plant nucleotide-binding site-leucine-rich repeat (NBS-LRR) genes. *New Phytol* **193:** 1049–1063.

Zimmermann, S., Nurnberger, T., Frachisse, J.-M., Wirtz, W., Guern, J., Hedrich, R., and Scheel, D. (1997) Receptor-mediated activation of a plant Ca2+-permeable ion channel involved in pathogen defense. *Proc Natl Acad Sci USA* **94:** 2751–2755.

Supporting information

Additional Supporting Information may be found in the online version of this article at the publisher's web-site:

Table S1. Differentially expressed genes in *Thalassiosira pseudonana* after 8 h of co-culture with *Ruegeria pomeroyi* DSS-3 relative to B_{12}-replete mono-culture (>twofold differential expression and fdr cutoff of <0.05; baySeq, Hardcastle and Kelly, 2010). Functional information is derived from Interpro, GO, Pfam and user annotations available for the *T. pseudonana* genome in the JGI Genome Portal.

Table S2. Differentially expressed genes in *Thalassiosira pseudonana* after 56 h of co-culture with *Ruegeria pomeroyi* DSS-3 relative to B_{12}-replete mono-culture (>twofold differential expression and fdr cutoff of <0.05; baySeq, Hardcastle and Kelly, 2010). Functional information is derived from Interpro, GO, Pfam and user annotations available for the *T. pseudonana* genome in the JGI Genome Portal.

Table S3. Results of BLAST analysis against the NCBI RefSeq database (release 77) of the leucine rich repeat (LRR) structural motif of upregulated *T. pseudonana* genes.

Table S4. Differentially expressed genes in *Ruegeria pomeroyi* DSS-3 after 8 h of co-culture with diatom *Thalassiosira pseudonana* relative to no-substrate controls (>twofold differential expression and an fdr <0.05 cutoff; baySeq, Hardcastle and Kelly, 2010). Functional information was derived from annotations at Roseobase (www.roseobase.org).

Figure S1. The ability of *Ruegeria pomeroyi* DSS-3 to grow on select organic carbon (C) and nitrogen (N) sources in *f*/2 (+Si, $-B_{12}$) medium, including sulfonates *N*-acetyltaurine (NAT) (which provides both carbon and nitrogen to the bacterium) and dihydroxypropanesulfonate (DHPS). Inset: *R. pomeroyi* requires addition of a usable nitrogen compound for growth in *f*/2 medium because it is unable to assimilate nitrate.

Figure S2. Putative orthologues of *T. pseudonana* LRR domain-containing protein Tp5595 (grey box) in the MMETSP marine microeukaryote transcriptome assemblies (http://marinemicroeukaryotes.org) (Keeling et al., 2014). Outgroups include related LRR-domain-containing proteins in *T. pseudonana*. See Methods for details of tree construction.

Figure S3. Putative orthologues of *T. pseudonana* LRR domain-containing protein Tp20707 (grey box) in the MMETSP marine microeukaryote transcriptome assemblies (http://marinemicroeukaryotes.org) (Keeling et al., 2014). Outgroups include related LRR-domain-containing proteins in *T. pseudonana*. See Methods for details of tree construction.

Figure S4. Putative orthologues of *T. pseudonana* LRR domain-containing protein Tp25675 (grey box) in the MMETSP marine microeukaryote transcriptome assemblies (http://marinemicroeukaryotes.org) (Keeling et al., 2014). Outgroups include related LRR-domain-containing proteins in *T. pseudonana*. See Methods for details of tree construction.

Figure S5. Following transfer of the *T. pseudonana* cultures into fresh medium after 150 h of growth, exponential growth resumed for both mono- and co-cultures.